

Exergy analysis of solid oxide fuel cell operating on natural gas

Kesavarapu Uma Sai Mahesh

A Thesis Submitted to
Indian Institute of Technology Hyderabad
In Partial Fulfillment of the Requirements for
The Degree of Master of Technology



भारतीय प्रौद्योगिकी संस्थान हैदराबाद
Indian Institute of Technology Hyderabad

Department of Chemical Engineering

June 2018

Declaration

I declare that this written submission represents my ideas in my own words, and where ideas or words of others have been included, I have adequately cited and referenced the original sources. I also declare that I have adhered to all principles of academic honesty and integrity and have not misrepresented or fabricated or falsified any idea/data/fact/source in my submission. I understand that any violation of the above will be a cause for disciplinary action by the Institute and can also evoke penal action from the sources that have thus not been properly cited, or from whom proper permission has not been taken when needed.

K. Uma Sai Mahesh

(Signature)

(Kesavarapu Uma Sai Mahesh)

CH16MTECH11009

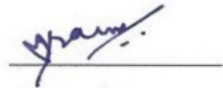
(Roll No.)

Approval Sheet

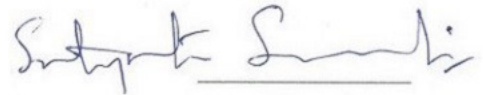
This Thesis entitled Exergy analysis of solid oxide fuel cell operating on natural gas by Kesavarapu Uma Sai Mahesh is approved for the degree of Master of Technology from IIT Hyderabad



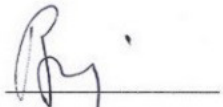
(Dr Vinod Janardhanan) Adviser
Dept. of Chem Engg
IITH



(Dr Praveen Meduri) Examiner
Dept. of Chem Engg
IITH



(Dr Satyavrata Samavedi) Examiner
Dept. of Chem Engg
IITH



(Dr Raja Banerjee) Chairman
External Examiner
Dept. of Mech Engg
IITH

Acknowledgements

It is great and immense pleasure that I have worked under the guidance of Dr. Vinod Janardhanan. I would like to express my sincere gratitude to my adviser Dr. Vinod Janardhanan for giving his guidance, assistance and suggestions throughout the project course. I felt really joyful to have a flexible advisor like him. Because of Dr. Vinod Janardhanan, an adept in fuel cell technology , I have improved my knowledge in the field of fuel cell technology.

I am also thankful to my thesis committee members Dr. Satyavrtaa Samavedi and Dr. Praveen Meduri for their valuable comments and suggestions.

I also thank my research group members (Vivek, Prakash and Swetha) for their support. I am very thankful to Mr. Prakash who helped me to understand the simulation better.

Dedication

To my parents and friends

Abstract

The fuel cell performance can be determined by various methods described in literature like impedance studies, cycle voltametry efficiency and exergy analysis etc,. In this work exergy analysis is implemented to study the performance of two types of fuel cells namely HT - PEMFC and SOFC. Exergy analysis can be used to determine not only the quantity of energy utilized but also the quality of the energy. Now a days exergy analysis is extensively used to determine the magnitude of energy loss and its location. In this work, exergy analysis is done on HT - PEMFC to identify the locations or equipments where loss of energy could be take place. This can be used to improve the overall performance of the system. In additional to the exergy analysis of HT-PEMFC, the performance of SOFC is also examined by exergy analysis. Assuming that all channels in a stack behave similarly, a single channel is simulated at different temperatures at different cell voltages and variable fuel composition. Also, SOFC is run at constant flow rate condition to validate the exergy analysis.

Contents

Declaration	ii
Approval Sheet	iii
Acknowledgements	iv
Abstract	vi
Nomenclature	viii
List of Tables	1
List of Figures	2
1 Fuel cell fundamentals	1
1.1 History	1
1.2 Types of fuel cells	2
1.3 Advantages and Disadvantages of fuel cells	3
1.4 Solid Oxide Fuel Cell	3
2 Exergy	5
2.1 Concept of Exergy	5
2.1.1 Types of Exergy	5
2.2 Physical exergy	6
2.2.1 Closed System Exergy balance	6
2.2.2 Open system exergy balance	7
2.3 Chemical Exergy	8
2.3.1 Reference Components from Air	8
2.3.2 Chemical Exergy of mixture	8
2.4 Exergy Efficiency of common components	9
2.4.1 Heat Exchanger without Mixing	9
2.4.2 Direct contact heat exchanger	10
3 HT - PEMFC	11
3.1 Polymer Electrolyte Membrane Fuel cell	11
3.2 High Temperature Polymer Electrolyte Membrane Fuel Cells	11
3.3 Model description	12
3.4 Exergy analysis	13

4 SOFC Model	19
5 Results and Discussion	22
5.1 Exergy efficiency	22
5.2 Efficiency at constant flow rate	27
5.3 Efficiency at constant stoichiometry	33
6 Conclusions	35
Bibliography	36

List of Tables

1.1	Types of fuel cells	2
1.2	Description of Fuel cell Types	3
1.3	Advantages and Disadvantages of Fuel cells	3
1.4	Advantages of Solid oxide fuel cell	4
2.1	Partial Pressures of components	8
2.2	Standard Chemical exergy values	9
3.1	Advantages and Disadvantages of PEMFC	11
3.2	Input flowrates of substances	13
3.3	Heat exchangers involved in the CHP System	13
3.4	Equipments involved chemical reactions in CHP system	14
3.5	NASA Polynomials for various species at low temperatures	15
3.6	NASA Polynomials for various species at high temperatures	15
3.7	Exergy analysis of various heat exchangers in the system	17
3.8	Exergy analysis of equipments involving chemical reactions	18
5.1	Velocities at different temperatures	27
5.2	Enthalpy change at different mole fractions	28

List of Figures

1.1	History of fuel cells	2
2.1	Counter flow heat exchanger	9
2.2	Direct contact heat exchanger	10
3.1	Layout of CHP system	12
3.2	Exergy efficiency of equipments in the CHP system	18
5.1	Exergy and Power distribution	23
5.2	Variation of mole fraction of H ₂ and CO with operating voltage	23
5.3	Variation of mole fraction of H ₂ O and CO ₂ with operating voltage	24
5.4	Variation of exergy efficiency with mole fraction of CH ₄ at 600 ⁰ C	25
5.5	Variation of exergy efficiency with mole fraction of CH ₄ at 700 ⁰ C	26
5.6	Variation of exergy efficiency with mole fraction of CH ₄ at 800 ⁰ C	26
5.7	Variation of exergy efficiency with temperature at 0.3 mole fraction of CH ₄	27
5.8	Efficiency at constant flow rate at 600 ⁰ C	29
5.9	Efficiency at constant flow rate at 700 ⁰ C	29
5.10	Efficiency at constant flow rate at 800 ⁰ C	30
5.11	Variation of fuel utilization at different mole fractions of CH ₄ at 600 ⁰ C	31
5.12	Variation of fuel utilization at different mole fractions of CH ₄ at 700 ⁰ C	31
5.13	Variation of fuel utilization at different mole fractions of CH ₄ at 800 ⁰ C	32
5.14	Efficiency at constant flow rate at different temperatures	33
5.15	Efficiency at constant stoichiometry condition at 800 ⁰ C	34

Chapter 1

Fuel cell fundamentals

1.1 History

Fuel cell technology was first developed in the year 1839 by Sir William Robert Grove [1]. Hydrogen and oxygen were mixed in an electrolyte to produce electricity. Earlier fuel cells were developed using platinum electrodes and sulphuric acid as the electrolyte. But, later sulphuric acid was replaced by other alkaline electrolytes due to its corrosive nature. The founder of the chemistry - physics, Friedrich Wilhelm Ostwald determined the interconnection of fuel cell components like electrodes, electrolyte, oxidizing and reducing agents [2]. In 1896, first fuel cell with practical applications was developed by William W. Jacques [3]. In 1900, Nernst used zirconium as solid electrolyte. In 1921, first molten carbonate fuel cell was built by Baur [4]. In 1959, fuel cell was used in 20 horsepower tractor successfully by Allis - Chalmers Manufacturing Company. In 1960s, fuel cells were used to produce electricity in NASA's Gemini and Apollo space crafts. In 1961, G.V.Elmore and H.A.Tanner developed a phosphoric acid fuel cell. In 1997, leading auto-mobile companies like Daimler - Benz and Toyota announced their project about fuel cell powered cars. In 2007, fuel cells were used for stationary backup power on commercial scale. In 2008, Daimler - Benz completed their projects about fuel cell powered cars [5]. Fuel cell technology was incorporated to run buses successfully. In 2009, micro - CHP units were sold in Japan. Fuel cell can be used in mobile phones and laptops. Motorola, Samsung, Sony have used fuel cells in telecommunication equipments [6]. Figure 1.1 represents the history of fuel cells [7].

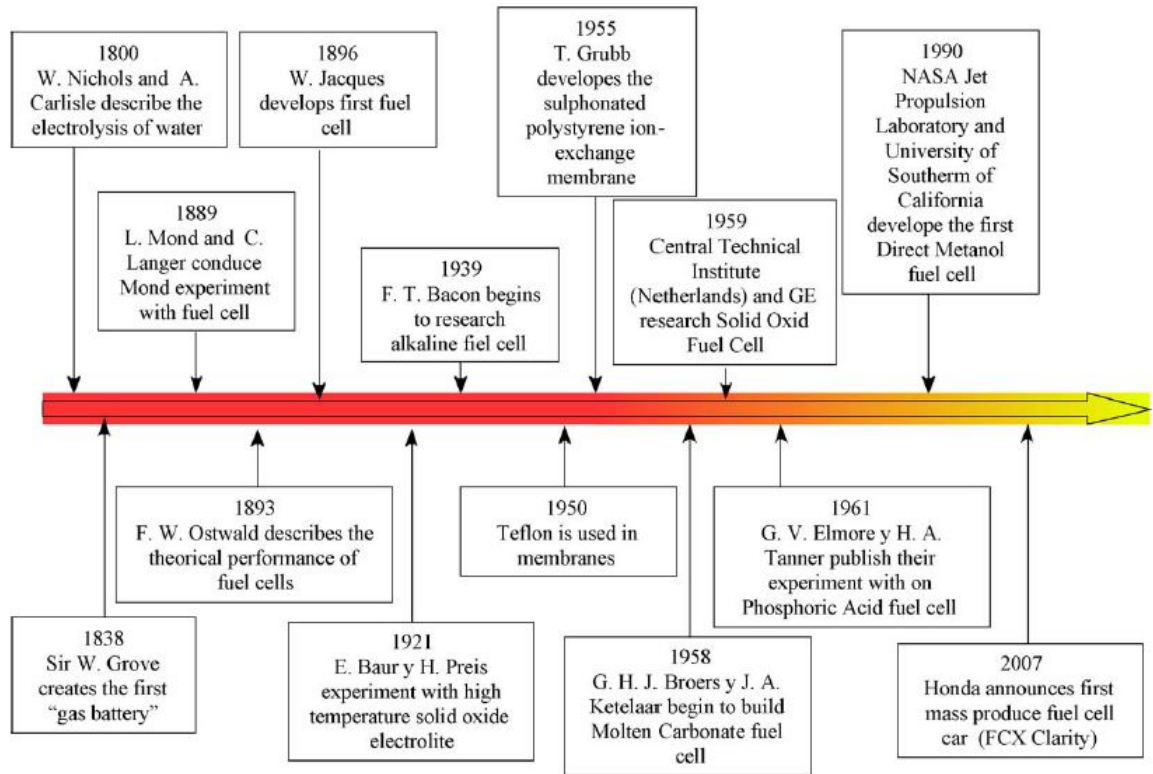


Figure 1.1: History of fuel cells

1.2 Types of fuel cells

Fuel cells are divided primarily into categories based on their electrolyte type. Based on this classification, types of electro - chemical reactions take place in various fuel cells are different. These fuel cells differ each other in various parameters: the type of catalyst involved, the operating temperature range, the requirement of fuel and the type of application. There are mainly five types of fuel cells available as shown in the Table 1.1.

Table 1.1: Types of fuel cells

S.No	Fuel cell type
1.	Polymer electrolyte membrane fuel cell (PEMFC)
2.	Phosphoric acid fuel cell (PAFC)
3.	Alkaline fuel cell (AFC)
4.	Molten carbonate fuel cell (MCFC)
5.	Solid oxide fuel cell (SOFC)

Table 1.2 shows a brief description of all types of fuel cells [8].

Table 1.2: Description of Fuel cell Types

S.No	Fuel cell	Electrolyte	Charge carrier	Operating temperature	Catalyst	Fuel
1.	PEMFC	Polymer membrane	H^+	$80^{\circ}C$	Platinum	H_2 , Methanol
2.	PAFC	Liquid H_3PO_4	H^+	$200^{\circ}C$	Platinum	H_2
3.	AFC	Liquid KOH	OH^-	$60 - 220^{\circ}C$	Platinum	H_2
4.	MCFC	Molten carbonate	CO_3^{2-}	$650^{\circ}C$	Nickel	H_2, CH_4
5.	SOFC	Ceramic	O^{2-}	$600-1000^{\circ}C$	Ceramic	H_2, CH_4, CO

1.3 Advantages and Disadvantages of fuel cells

Fuel cell technology is a viable option to produce power due to its advantages over its counterparts like batteries and combustion engines. Energy density of fuel cells is much more than batteries. Table 1.3 shows advantages and disadvantages of fuel cell technology [9, 10].

Table 1.3: Advantages and Disadvantages of Fuel cells

S.No	Advantages	Disadvantages
1.	Simplicity in design	Expensive
2.	Low emission	Fuel availability and storage
3.	Silent operation	Limitation on operation temperature
4.	High efficiency	Durability during start-up

1.4 Solid Oxide Fuel Cell

When compared to different types of fuel cells, solid oxide fuel cell has advantages in terms of operating temperature, fuel choice and components involved. Solid oxide fuel cells are typically operated at the temperature range of $600^{\circ}C - 1000^{\circ}C$. The electrolyte is in solid phase. So vigorous water management systems can be avoided. Due to high operating temperature, internal reforming of fuel can also be achieved within the cell which eliminate expensive set-up for reformation outside the cell. Also, high temperature operation allows to produce useful heat for co-generation and to construct hybrid systems. They are resistant to various impurities present in the fuel like carbon monoxide. Carbon monoxide can be used as fuel in this type of fuel cells. This made them to use natural gas, biogas and gases from coal as fuel. Table 1.4 shows advantages of Solid oxide fuel cell [10].

Table 1.4: Advantages of Solid oxide fuel cell

S.No	Advantages
1.	High operation temperature
2.	No electrolyte loss
3.	No need of expensive catalysts
4.	Ability to handle impurities
5.	Internal reforming ability
6.	High quality waste heat for co-generation

Solid oxide fuel cells have disadvantages too. High temperature operation leads to slow start-up. It requires stringent durability requirements on materials. One of the key challenge in this type of fuel cells is development of low cost materials with high durability. For this reason development of lower - temperature SOFCs operating at 600°C to 700°C are being researched. This low temperature operation ensures fewer durability problems and less cost.

Chapter 2

Exergy

2.1 Concept of Exergy

It is essential to find out the efficiency of fuel cells either using thermodynamic efficiency or exergy efficiency. Methods based on the thermodynamics give the detailed information about the magnitude of losses within the cells. One of the methods which is based on the thermodynamics is concept of exergy. Efficiency based on the first law of thermodynamics gives information about quantity of the energy. On the other hand Exergy which is based on the second law of thermodynamics gives not only the quantity but also about quality of the energy.

Exergy concept was demonstrated by Gibbs in 1878. It was developed by Rant in 1957. Exergy is defined as the maximum amount of work obtained when the system comes to equilibrium while interacting with the environment. Environment is considered as large and uniform at the temperature T_0 and the pressure P_0 . For the analysis of exergy the temperature and pressure of environment is considered to be constant at 25°C and at 1 atm.

When the system reaches the state of environment, there is still a chance to extract the work because of difference in the quantity of matter between the system and the environment even-though the system is at environmental state. A state which is reached when work is extracted as the matter is equilibrated with the environment is called as dead state.

2.1.1 Types of Exergy

There are several types of exergies and the total exergy is defined as

$$\mathbf{E} = \mathbf{E}_{\text{ki}} + \mathbf{E}_{\text{po}} + \mathbf{E}_{\text{ph}} + \mathbf{E}_{\text{ch}}. \quad (2.1)$$

Where \mathbf{E}_{ki} , \mathbf{E}_{po} , \mathbf{E}_{ph} and \mathbf{E}_{ch} are kinetic, potential, physical and chemical exergies respectively.

Exergy of a system is given by

$$\mathbf{E} = (E - U_0) + P_0(V - V_0) - T_0(S - S_0). \quad (2.2)$$

Where $E(=U+KE+PE)$, V and S are energy, volume and entropy of the system respectively.

The specific exergy on a unit mass basis, e , is given by

$$\mathbf{e} = (e - u_0) + p_0(v - v_0) - T_0(s - s_0). \quad (2.3)$$

Where e , v and s are the specific energy, volume and entropy of the system respectively. u_0 , v_0 and s_0 are evaluated at the dead state. With $e = u + \frac{V^2}{2} + gz$,

$$e = \left[\left(u + \frac{V^2}{2} + gz \right) - u_0 \right] + p_0(v - v_0) - T_0(s - s_0) \quad (2.4)$$

. The above equation can be rewrite as

$$e = (u - u_0) + p_0(v - v_0) - T_0(s - s_0) + \frac{V^2}{2} + gz. \quad (2.5)$$

In general kinetic and potential exergies are omitted and physical and chemical exergies are considered for the calculations.

The change in exergy between two states is given by

$$\mathbf{E}_2 - \mathbf{E}_1 = (E_2 - E_1) + p_0(V_2 - V_1) - T_0(S_2 - S_1). \quad (2.6)$$

2.2 Physical exergy

Physical exergy is defined as the maximum work is produced when the systme is brought from initial state (T, P) to the environmental state (T_0, P_0) . The processes that are considered to be involved in the physical exergy are physical processes involves only thermal interactions with the environment.

2.2.1 Closed System Exergy balance

In a closed system, transfer of energy between system and the environment occurs without exchanging the matter. The exergy balance involves formation of energy and entropy across the boundary.

The energy and entropy balances are given by

$$E_2 - E_1 = \int_1^2 \delta Q - W, \quad (2.7)$$

$$S_2 - S_1 = \int_1^2 \left(\frac{\delta Q}{T} \right) + \sigma. \quad (2.8)$$

Where W and Q represent work and heat transfers between the system and the surroundings. T , δQ and σ represent temperature of the system, amount of heat received and entropy generation.

Exergy balance for closed system is given by

$$(E_2 - E_1) - T_0(S_2 - S_1) = \int_1^2 \delta Q - T_0 \int_1^2 \left(\frac{\delta Q}{T} \right) - W - T_0 \sigma. \quad (2.9)$$

Introducing Eq.2.6 on the left side, we can get

$$(\mathbf{E}_2 - \mathbf{E}_1) - p_0(V_2 - V_1) = \int_1^2 \left(1 - \frac{T_0}{T} \right) \delta Q - W - T_0 \sigma, \quad (2.10)$$

$$\underbrace{\mathbf{E}_2 - \mathbf{E}_1}_{\text{amount of exergy}} = \underbrace{\int_1^2 \left(1 - \frac{T_0}{T}\right) \delta Q}_{\text{exergy related to heat}} - \underbrace{W - p_0(V_2 - V_1)}_{\text{exergy related to work}} - \underbrace{T_0 \sigma}_{\text{exergy destruction}} \quad (2.11)$$

In the rate form, it is

$$\underbrace{\frac{d\mathbf{E}}{dt}}_{\text{rate of change of exergy}} = \underbrace{\sum_j \left(1 - \frac{T_0}{T}\right) \dot{Q}_j}_{\text{rate of change of exergy due to heat transfer}} - \underbrace{\left(\dot{W} - p_0 \frac{dV}{dt}\right)}_{\text{rate of change of volume of system}} - \underbrace{\dot{\mathbf{E}}_d}_{\text{rate of exergy destruction}} \quad (2.12)$$

2.2.2 Open system exergy balance

Open system is defined as transfer of not only energy but also the matter between system and the environment.

Specific flow exergy is given by

$$e_f = h - h_0 - T_0(s - s_0) + \frac{V^2}{2} + gz. \quad (2.13)$$

Where h and s represent the specific enthalpy and entropy of the system respectively. h_0 and s_0 are evaluated at the dead state. f stands for flow.

Exergy balance for control volume is

$$\underbrace{\frac{d\mathbf{E}}{dt}}_{\text{rate of exergy change}} = \underbrace{\sum_j \left(1 - \frac{T_0}{T_j}\right) \dot{Q}_j - \left(\dot{W} - p_0 \frac{dV}{dt}\right) + \sum_i \dot{m}_i e_{fi} - \sum_e \dot{m}_e e_{ef}}_{\text{rate of exergy transfer}} - \underbrace{\dot{\mathbf{E}}_d}_{\text{rate of exergy destruction}} \quad (2.14)$$

Where i , e , \dot{m} and j denote inlet, exit, mass flow rate and location on the boundary respectively. Steady - state form is

$$0 = \sum_j \left(1 - \frac{T_0}{T_j}\right) \dot{Q}_j - \dot{W} + \sum_i \dot{m}_i e_{fi} - \sum_e \dot{m}_e e_{fe} - \dot{\mathbf{E}}_d. \quad (2.15)$$

For one inlet and one outlet, it becomes

$$0 = \sum_j \left(1 - \frac{T_0}{T_j}\right) \dot{Q}_j - \dot{W} + \dot{m}(e_{f1} - e_{f2}) - \dot{\mathbf{E}}_d. \quad (2.16)$$

Where,

$$e_{f1} - e_{f2} = (h_1 - h_2) - T_0(s_1 - s_2) + \frac{V_1^2 - V_2^2}{2} + g(z_1 - z_2). \quad (2.17)$$

If the velocities at the both ends are almost same and there is no elevation then

$$e_{f1} - e_{f2} = (h_1 - h_2) - T_0(s_1 - s_2), \quad (2.18)$$

or generally at one location

$$\mathbf{E}_{ph} = (h - h_0) - T_0(s - s_0). \quad (2.19)$$

The above equation is treated as physical exergy.

For Ideal gaseous mixture,

the enthalpy depends only on the temperature as follows

$$h - h_0 = \int_{T_0}^T c_p dT. \quad (2.20)$$

The entropy change is given by

$$s - s_0 = \int_{T_0}^T c_p \frac{dT}{T} - R \int_{p_0}^p \frac{dp}{p}, \quad (2.21)$$

$$s - s_0 = \int_{T_0}^T c_p \frac{dT}{T} - R \ln \frac{p}{p_0}. \quad (2.22)$$

For constant values of c_p ,

$$\mathbf{E}_{ph} = c_p(T - T_0) - T_0 c_p \ln \frac{T}{T_0} + RT_0 \ln \frac{p}{p_0}. \quad (2.23)$$

Where c_p represents specific heat capacity. T and p represent temperature and pressure of the system. T_0 and p_0 represents standard temperature and pressure respectively.

2.3 Chemical Exergy

Chemical exergy is defined as the maximum amount of work is produced when the system is brought from the environmental state to the dead state. The chemical exergy is related to the departure of the chemical composition of a system from that of the environment. To determine the chemical exergy of species present in the system we need to define the proper reference environment. Generally this reference environment is taken as the atmosphere, the oceans and the earth's crust at the temperature T_0 and pressure P_0 .

2.3.1 Reference Components from Air

The main components of air are O_2 , N_2 , CO_2 and H_2O , at 298.15K and 1 atm. Table 2.1 shows partial pressure of these components [11].

Table 2.1: Partial Pressures of components

Component	Partial pressure(kPa)
N_2	75.78
O_2	20.39
CO_2	0.0335
H_2O	2.2

2.3.2 Chemical Exergy of mixture

The chemical exergy of the mixture can be calculated once the chemical exergy of all the substances present in the process is obtained. Specific chemical exergy depends on the streams composition,

for calculation of chemical exergy of the stream we need the information about the specific chemical exergy of the substances and their molar fractions.

For gas mixtures and ideal liquid solutions the formula is given by [12],

$$\mathbf{E}_{\text{ch}} = \sum_i x_i e_{\text{ch},i} + RT_0 \sum_i x_i \ln x_i. \quad (2.24)$$

where $e_{\text{ch},i}$, x_i are specific chemical exergy of i^{th} substance and mole fraction of substance in the mixture respectively.

The Standard Chemical Exergy Values of components are listed in Table 2.2 [13].

Table 2.2: Standard Chemical exergy values

Component	Standard Chemical exergy, $e_{\text{ch},i}$ (kJ/mol)
CH ₄	831.2
H ₂ O	9.5
H ₂	236.09
O ₂	3.97
N ₂	0.72
CO ₂	19.48
CO	274.71

2.4 Exergy Efficiency of common components

2.4.1 Heat Exchanger without Mixing

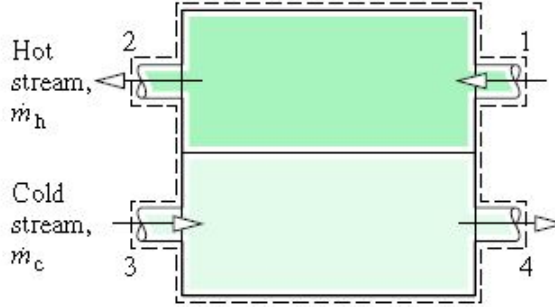


Figure 2.1: Counter flow heat exchanger

Figure 2.1 represents a counter flow heat exchanger [14]. The mass flow rate of hot stream is \dot{m}_h and that of cold stream is \dot{m}_c . Assume that the heat exchanger is at steady state with no heat transfer with the environment. The rate of change of exergy balance is given as

$$0 = \sum_j \left(1 - \frac{T_0}{T}\right) \dot{Q}_j - \dot{W} + (\dot{m}_h e_{f1} + \dot{m}_c e_{f3}) - (\dot{m}_h e_{f2} + \dot{m}_c e_{f4}) - \dot{E}_d, \quad (2.25)$$

$$\dot{m}_h(e_{f1} - e_{f2}) = \dot{m}_c(e_{f4} - e_{f3}) + \dot{\mathbf{E}}_d. \quad (2.26)$$

The exergy efficiency of heat exchanger is given as

$$\varepsilon = \frac{\dot{m}_c(e_{f4} - e_{f3})}{\dot{m}_h(e_{f1} - e_{f2})}. \quad (2.27)$$

2.4.2 Direct contact heat exchanger

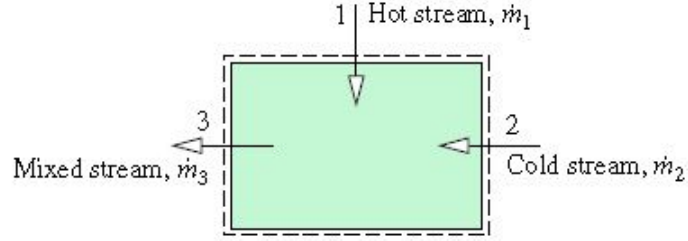


Figure 2.2: Direct contact heat exchanger

Figure 2.2 represents a mixer with two streams flowing into the system and after mixing one stream leaving the system [14]. The exergy balance is given as

$$0 = \sum_j \left(1 - \frac{T_0}{T}\right) \dot{Q}_j - \dot{W} + \dot{m}_1 e_{f1} - \dot{m}_3 e_{f3} - \dot{\mathbf{E}}_d, \quad (2.28)$$

and

$$\dot{m}_3 = \dot{m}_1 + \dot{m}_2. \quad (2.29)$$

Therefore the equation is reduced to

$$\dot{m}_1(e_{f1} - e_{f3}) = \dot{m}_2(e_{f3} - e_{f2}) + \dot{\mathbf{E}}_d. \quad (2.30)$$

The exergy efficiency is given as

$$\varepsilon = \frac{\dot{m}_2(e_{f3} - e_{f2})}{\dot{m}_1(e_{f1} - e_{f3})}. \quad (2.31)$$

Chapter 3

HT - PEMFC

3.1 Polymer Electrolyte Membrane Fuel cell

Polymer Electrolyte Membrane Fuel cells(PEMFC) are operable in the temperature range from 80⁰C to 200⁰C. These fuel cells mainly use H₂ as fuel. These cells are best for transport, mobile auxiliary and combined heat and power (CHP) applications. These are first choice for transport industry because of their rapid start-up, high power density and efficiency. There are two types of PEMFC's. Low Temperature Polymer Electrolyte Membrane Fuel cells(LT-PEMFC) and High Temperature Polymer Electrolyte Membrane Fuel cells(HT-PEMFC).

Low temperature Polymer Electrolyte Membrane Fuel cells are operated at 80⁰C. They suffer from number of disadvantages mainly low tolerance to impurities and water management. By switching to high temperature Polymer Electrolyte Membrane Fuel cells the above mentioned difficulties can be mitigated.

3.2 High Temperature Polymer Electrolyte Membrane Fuel Cells

HTPEMFC are operable upto 200⁰C with improved kinetics which lead to improved performance compared to LTPEMFC. Table 3.1 provides advantages and disadvantages of HTPEMFC [15, 16].

Table 3.1: Advantages and Disadvantages of PEMFC

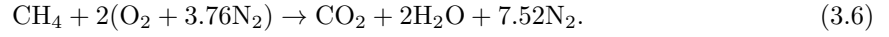
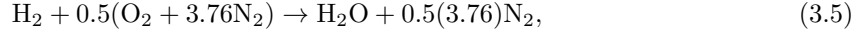
S.NO.	Advantages	Disadvantages
1.	Improved reaction kinetics	Dehydration of membrane
2.	CO tolerance	Increased start-up time
3.	Heat and water management	Acid leaching
4.	Use of alternative catalysts	Durability



WGS reactor:



Combustor:



Fuel cell stack:



3.4 Exergy analysis

The inputs to the system are natural gas, water and air at various points. The input temperature and flow rates are shown in the Table 3.2.

Table 3.2: Input flowrates of substances

S.No.	Component	Temperature (K)	flowrate (Kg/s)
1.	Natural gas	288	7.31E-05
2.	Water	293	1.10E-02
3.	Air	288	6.50E-03

The exergy analysis of the equipments involves the calculation of the enthalpy and entropy at the inlet and outlet conditions which depends on temperature and pressure. By knowing the temperature and pressure at the inlet and outlet of the each and every equipment we can calculate physical exergy (Eq. 2.12) and chemical exergy (Eq. 2.17) depending on the type of process involved in the equipment.

The types of heat exchangers involved in the system are shown in Table 3.3

Table 3.3: Heat exchangers involved in the CHP System

S.No	Equipment Name	Equipment Type
1.	Natural gas preheater	Indirect contact heat exchanger
2.	Steam generator	Indirect contact heat exchanger
3.	SMR/WGS Cooler	Indirect contact heat exchanger
4.	WGS/HT - PEMFC Cooler	Indirect contact heat exchanger
5.	1 st cogeneration	Indirect contact heat exchanger
6.	2 nd cogeneration	Indirect contact heat exchanger
7.	3 rd cogeneration	Indirect contact heat exchanger
8.	Mixer	Direct contact heat exchanger

The remaining equipments are shown in Table 3.4.

Table 3.4: Equipments involved chemical reactions in CHP system

S.No	Equipment Name
1.	Combustor
2.	SMR reactor
3.	WGS reactor
4.	Fuel cell stack

The enthalpy and entropy values of various species involved in the system are calculated based on the NASA Polynomials as shown in Table 3.5 and Table 3.6 for low temperatures (below 1000⁰C) and high temperatures (above 1000⁰C) respectively.

Table 3.5: NASA Polynomials for various species at low temperatures

Constant	CH ₄	H ₂ O	CO ₂	CO	H ₂	O ₂	N ₂
a_1	5.14911468	4.1986352	2.356813	3.5795335	2.3443029	3.78245636	3.53100528
a_2	-0.013662201	-0.002036402	0.00898413	-0.000610354	0.007980425	-0.002996734	-0.000123661
a_3	4.91424E-05	6.52034E-06	-7.12206E-06	1.01681E-06	-1.94779E-05	9.8473E-06	-5.02999E-07
a_4	-4.84247E-08	-5.48793E-09	2.4573E-09	9.07006E-10	2.0157E-08	-9.6813E-09	2.4353E-09
a_5	1.66603E-11	1.77197E-12	-1.42885E13	-9.04424E-13	-7.37603E-12	3.24373E-12	-1.40881E-12
a_6	-10246.5983	-30293.726	-48371.971	-14344.086	-917.92413	-1063.94356	-1046.97626
a_7	1.66603E-11	-0.84900901	9.9009035	3.5084093	0.68300218	3.65767573	2.96747038

Table 3.6: NASA Polynomials for various species at high temperatures

Constant	CH ₄	H ₂ O	CO ₂	CO	H ₂	O ₂	N ₂
a_1	1.65326226	2.6770389	4.6365111	3.0484859	2.9328305	3.66096083	2.95257637
a_2	0.01002631	0.002973182	0.00274157	0.001351728	0.000826598	0.000656366	0.0013969
a_3	-3.31661E-06	-7.73769E-07	-9.95898E-07	-4.85794E-07	-1.46401E-07	-1.41149E-07	-4.92632E-07
a_4	5.36483E-10	9.44335E-11	1.60387E-10	7.88536E-11	1.54099E-11	2.05798E-11	7.8601E-11
a_5	-3.14697E-14	-4.269E-15	-9.16199E-15	-4.69807E-15	-6.88796E-16	-1.29913E-15	-4.60755E-11
a_6	-10009.5936	-29885.894	-49024.904	-14266.117	-813.05582	-1215.97725	-923.948688
a_7	9.90506283	6.88255	-1.9348955	6.017099	-1.0243164	3.41536184	5.87188762

From the NASA Polynomials enthalpy and entropy values are calculated and total exergy is calculated at both ends by combining physical and chemical exergies. The exergy efficiency is calculated based on the Eq. 2.20 for indirect contact heat exchanger. Direct contact heat exchanger exergy efficiency is calculated based on the Eq. 2.20 and Eq. 2.24. The exergy analysis of various heat exchangers in the system is shown in Table 3.7 and exergy analysis of equipments involving chemical reactions is shown in Table 3.8.

Table 3.7: Exergy analysis of various heat exchangers in the system

S.No	Equipment Name	Cold fluid			Hot fluid				$\varepsilon = \frac{\dot{m}_c(e_{co}-e_{ci})}{\dot{m}_h(e_{hi}-e_{ho})}$	
		Flow rate (Kg/s)	Inlet temper- ature (K)	Outlet temper- ature (K)	Exergy (kW)	Flow rate (Kg/s)	Inlet temper- ature (K)	Outlet temper- ature (K)		Exergy (kW)
1.	NG Preheater	4.65E-05	298	399	1.56E-03	4.95E-03	561	559	5.68E-03	27.47
2.	Steam generator	2.09E-04	293	473	1.49E-02	4.95E-03	653	561	2.47E-01	06.01
3.	SMR/WGS Cooler	4.88E-03	385	432	5.09E-02	2.56E-04	1047	523	5.59E-02	21.05
4.	WGS/HT-PEMFC Cooler	4.88E-03	288	385	5.09E-02	3.23E-04	599	433	5.59E-02	91.00
5.	1 st Cogeneration	3.00E-03	293	333	2.06E-02	4.95E-03	559	516	1.05E-01	19.63
6.	2 nd Cogeneration	8.80E-03	293	333	3.10E-02	4.95E-03	516	299	2.80E-01	11.08
7.	3 rd Cogeneration	1.80E-03	293	367	2.20E-02	1.76E-03	433	305	4.59E-02	48.06
8.	Mixer	4.65E05	399	456	2.10E-03	2.09E-04	473	456	2.46E-03	85.32

Table 3.8: Exergy analysis of equipments involving chemical reactions

S.No	Equipment Name	Natural gas flow rate (Kg/s)	Depleted fuel (kW)	Preheated Air (kW)	Chemical Exergy (kW)	Reactants (kW)	Hot flue gases (kW)	Exergy Efficiency
1.	Combustor	5.86E-06	0.01	0.60153	2.4685	3.08003	2.8168	91.45

S.No	Equipment Name	Cold fluid	Chemical(cold fluid)	Total (cold fluid)	Flue gases	Exergy Efficiency
1.	SMR	3.19E-01	5.77E-01	8.96E-01	2.13E+00	41.99

S.No	Equipment Name	Reactants	Products	Exergy Efficiency
1.	WGS	9.08E-02	7.43E-02	81.77

S.No	Equipment Name	Reactants	Products	Power	Exergy Efficiency
1.	Fuel cell	1.78E+00	1.41E-01	6.16E-01	37.45

The exergy efficiency of various equipments in the CHP system are shown in the Fig. 3.2.

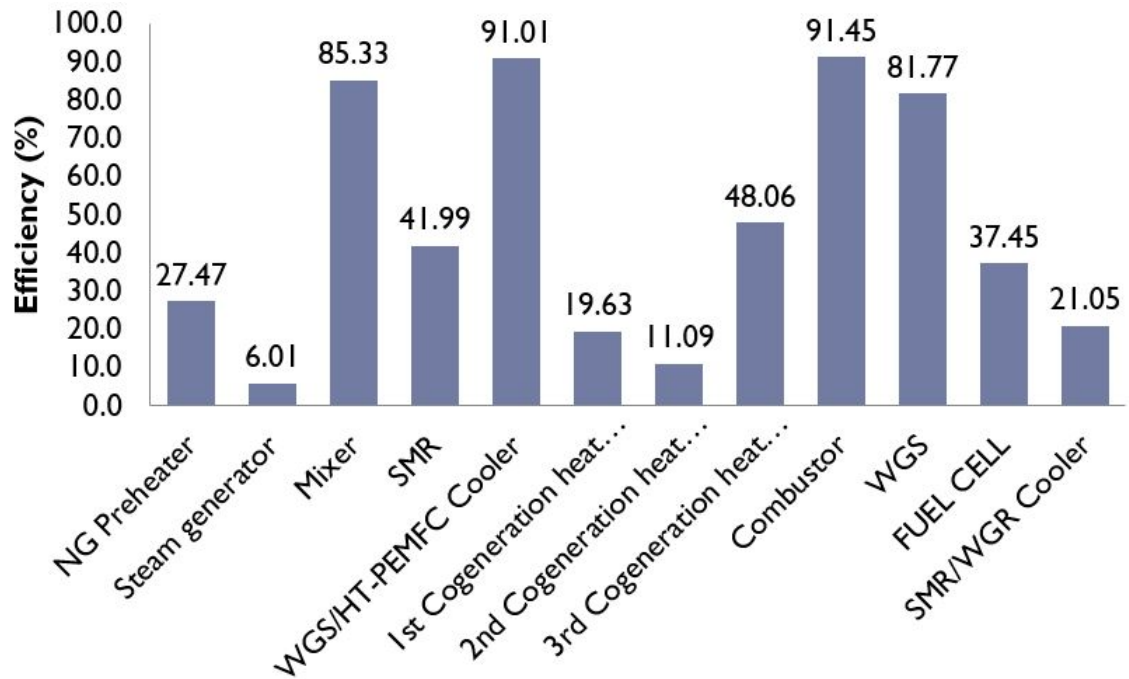


Figure 3.2: Exergy efficiency of equipments in the CHP system

Chapter 4

SOFC Model

The SOFC model considered here is planar configuration. The code consists of following files to execute the code: cloud.xml, chem.inp, ch4.xml, electrochem.xml and therm.dat. Assuming that all channels in a stack behave similarly, a single channel is simulated. A mixture of methane and water is considered as the fuel. In the SOFC, the following overall reaction is taken place.



The model is simulated at different mole fractions of CH_4 by varying operating voltage. The model is simulated at constant flow rate condition. In constant flow rate condition, a constant amount of fuel is supplied to the cell regardless of how much it actually needs at given current density.

The geometrical model considered in this work is single channel. The species mass fractions Y_k in the flow channels are calculated from [18]

$$\frac{\partial(\rho Y_k)}{\partial t} + \frac{\partial(\rho u Y_k)}{\partial x} = \frac{P_e}{A_c} j_k; k = 1 \dots N_g. \quad (4.2)$$

And the velocity is calculated from

$$\frac{\partial(\rho u)}{\partial t} + \frac{\partial(\rho u u)}{\partial x} = u \sum_{k=1}^{N_g} \frac{P_e}{A_c} j_k. \quad (4.3)$$

The pressure in the channel is assumed to be constant at atmospheric. The density then follows from the ideal gas equation is

$$\rho = \frac{p\bar{M}}{RT}. \quad (4.4)$$

In the above equations j_k is the flux at the interface between the flow channel and the electrode, which is calculated using

$$\frac{j_k}{M_k} = \sum_{l=1}^{N_g} d_{kl}^{\text{DGM}} \frac{C_l}{d_{l,Kn}^e} \frac{B_g}{\mu} \nabla p. \quad (4.5)$$

Here d_{kl}^{DGM} is DGM diffusion coefficients, which is defined as $d_{kl}^{\text{DGM}} = \mathbf{H}^{-1}$ and \mathbf{H} matrix is defined as

$$h_{kl} = \left(\frac{1}{d_{k,Kn}^e} + \sum_{j \neq k} \frac{X_j}{D_{kj}^e} \right) \delta_{kl} + (\delta_{kl} - 1) \frac{X_k}{d_{kl}^e}. \quad (4.6)$$

The permeability B_g is calculated using Kozeny - Carman equation

$$B_g = \frac{\epsilon^2 d_p^2}{72\tau(1 - \epsilon)^2}. \quad (4.7)$$

The viscosity and binary diffusion coefficient are calculated using the kinetic theory of gases. The effective diffusion coefficients are defined as

$$d_{k,Kn}^e = \frac{\epsilon}{\tau} d_{k,Kn}, \quad (4.8)$$

$$d_{kl}^e = \frac{\epsilon}{\tau} d_{kl}. \quad (4.9)$$

While flowing along the channels, the fuel and the oxidant species are transported into the GDL and CL by a combination of molecular and Knudsen diffusion. The species mass fraction Y_k in the electrodes is given by

$$\frac{\partial(\epsilon\rho Y_k)}{\partial t} = \frac{\partial j_k}{\partial y}; k = 1 \dots N_g. \quad (4.10)$$

The total density within the porous electrodes then follows

$$\frac{\partial(\epsilon\rho)}{\partial t} = \sum_{k=1}^{N_g} \frac{\partial j_k}{\partial y}. \quad (4.11)$$

The cell voltage is calculated according to

$$E_{cell} = E_{rev} - \eta_a(i) - |\eta_c(i)| - \eta_{ohm}(i). \quad (4.12)$$

Where E_{rev} , $\eta_a(i)$, $\eta_c(i)$ and $\eta_{ohm}(i)$ are reversible potential, anodic overpotential, cathodic overpotential and ohmic overpotential respectively. The reversible potential E_{rev} is calculated according to Nernst equation. We assume that the hydrogen electro - oxidation pathway is dominant, and so the reversible cell potential may be computed using the Nernst equation for the hydrogen oxidation reaction is given by

$$E_{rev} = E^0 + \frac{RT}{2F} \ln \left(\frac{p_{H_2,a}}{p_{H_2O,a}} \right) + \frac{RT}{2F} \ln \left(p_{O_2,c}^{1/2} \right). \quad (4.13)$$

where

$$E^0 = \frac{1}{2F} \left(\mu_{H_2}^0 + \frac{1}{2} \mu_{O_2}^0 - \mu_{H_2O}^0 \right) \quad (4.14)$$

is the ideal standard potential and μ_k^0 are standard - state chemical potentials. As indicated by the subscripts a and c, the gas phase species partial pressures are evaluated at the anode and cathode interfaces with the dense electrolyte. The current density can be written in a Butler - Volmer form as

$$i = i_0 \left[\exp \left(\frac{(\beta_a + 1)F\eta_a}{RT} \right) - \exp \left(-\frac{(\beta_c F\eta_a)}{RT} \right) \right]. \quad (4.15)$$

Where, $\eta_a = E_a - E_a^{eq}$ is the activation overpotential and the exchange current density is given as

$$i_0 = i_{H_2}^* \frac{(p_{H_2}/p_{H_2}^*)^{1/4} (p_{H_2O})^{3/4}}{1 + (p_{H_2}/p_{H_2}^*)^{1/2}}, \quad (4.16)$$

$$i = i_0 \left[\exp\left(\frac{(\beta_a + 1)F\eta_c}{RT}\right) - \exp\left(-\frac{(\beta_c F\eta_c)}{RT}\right) \right], \quad (4.17)$$

$$i_0 = i_{O_2}^* \frac{(p_{O_2}/p_{O_2}^*)^{1/4}}{1 + (p_{O_2}/p_{O_2}^*)^{1/2}}. \quad (4.18)$$

Chapter 5

Results and Discussion

The fuel cell stack is simulated at different temperatures, different operating potentials and different mole fractions of CH₄. Exergy analysis of SOFC will be discussed first. The results of efficiency at constant flow rate will then be presented to validate the exergy analysis. Finally efficiency at constant stoichiometry will be discussed.

5.1 Exergy efficiency

Fuel cells convert chemical energy in the fuel into the electrical output through electro-chemical reaction along with products. In order to determine the exergy efficiency we need to calculate the exergy of reactants as well as products. The exergy efficiency of the fuel cell is given by [12]

$$\varepsilon = \frac{\mathbf{P}}{\mathbf{E}_{\mathbf{R}} - \mathbf{E}_{\mathbf{P}}}. \quad (5.1)$$

Where \mathbf{P} , $\mathbf{E}_{\mathbf{R}}$ and $\mathbf{E}_{\mathbf{P}}$ are power extracted from the fuel cell, exergy of reactants and exergy of products respectively. The exergy of reactants and products are calculated using Eq. 2.19 and Eq. 2.24.

Variation of power (\mathbf{P}), exergy of reactants ($\mathbf{E}_{\mathbf{R}}$) and exergy of products ($\mathbf{E}_{\mathbf{P}}$) with operating voltage (V) is shown in Fig. 5.1.

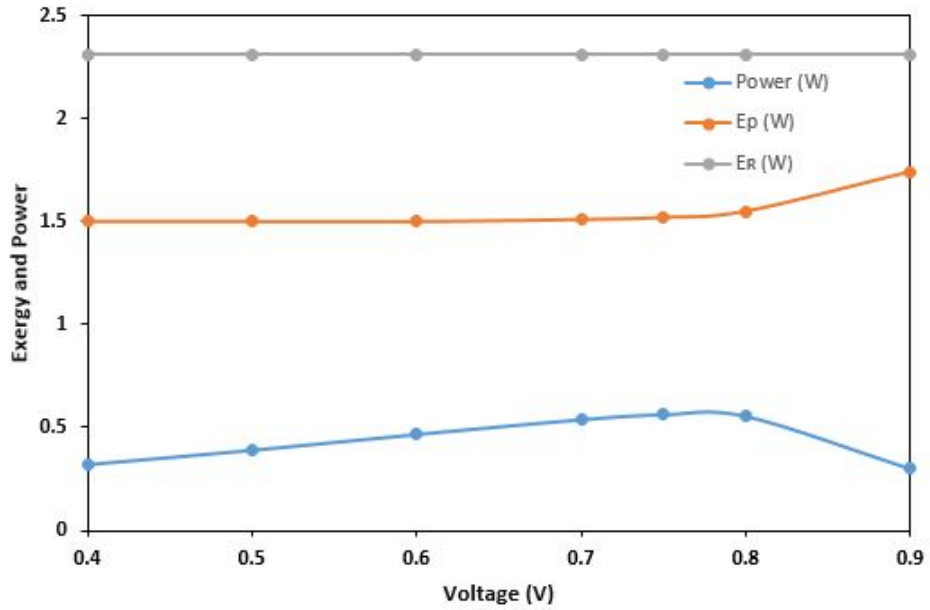


Figure 5.1: Exergy and Power distribution

Even though it is plotted at 800°C and CH_4 mole fraction of 0.3 in the fuel, the general trend is same at every temperature and for every mole fraction of CH_4 . From the Figure 5.1, it is clear that power produced reaches maximum and then decreases as the operating voltage increases. On the other hand, exergy of products increases continuously with operating voltage due to two factors: Increase of mole fraction of H_2 and CO and decrease of mole fraction of H_2O and CO_2 with operating voltage as shown in Fig. 5.2 and Fig. 5.3 respectively.

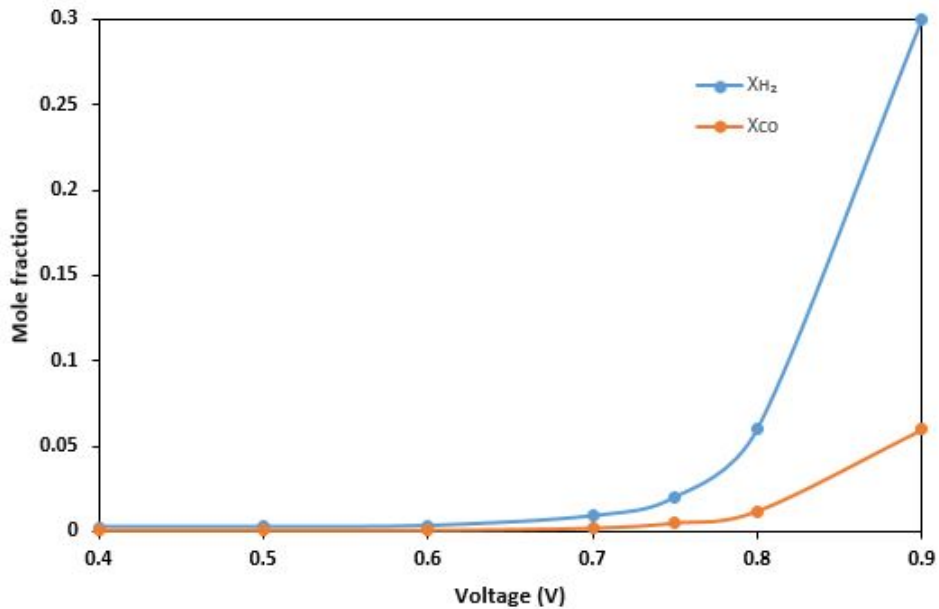


Figure 5.2: Variation of mole fraction of H_2 and CO with operating voltage

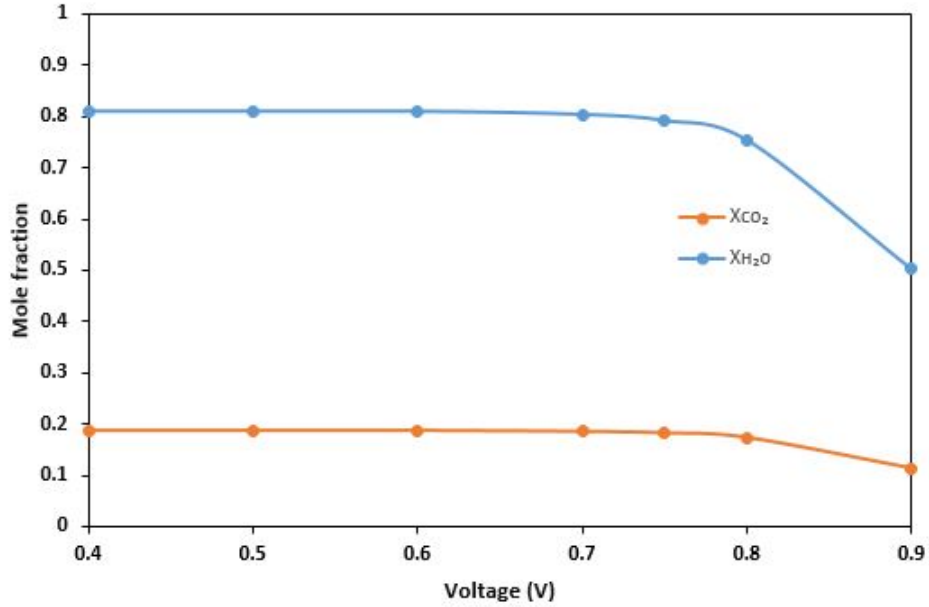


Figure 5.3: Variation of mole fraction of H₂O and CO₂ with operating voltage

The change in mole fraction of species is insignificant upto 0.7V. After 0.7V, mole fraction of H₂ and CO increases rapidly due to reduction in electro-chemical reaction of H₂. This leads to decrease of water formation and hence reduction in mole fraction of H₂O. It is already stated that exergy efficiency is combination of both physical exergy and chemical exergy. The chemical exergies of H₂ and CO are almost 25 times that of H₂O. This causes increase of products exergy and exergy efficiency also changes accordingly.

Exergy analysis is done at three different temperatures and three different mole fractions of CH₄. The three different temperatures considered at 600⁰C, 700⁰C and 800⁰C and 0.3, 0.5 and 0.7 mole fractions of CH₄.

The exergy efficiency of SOFC at 600⁰C is shown in Fig. 5.4.

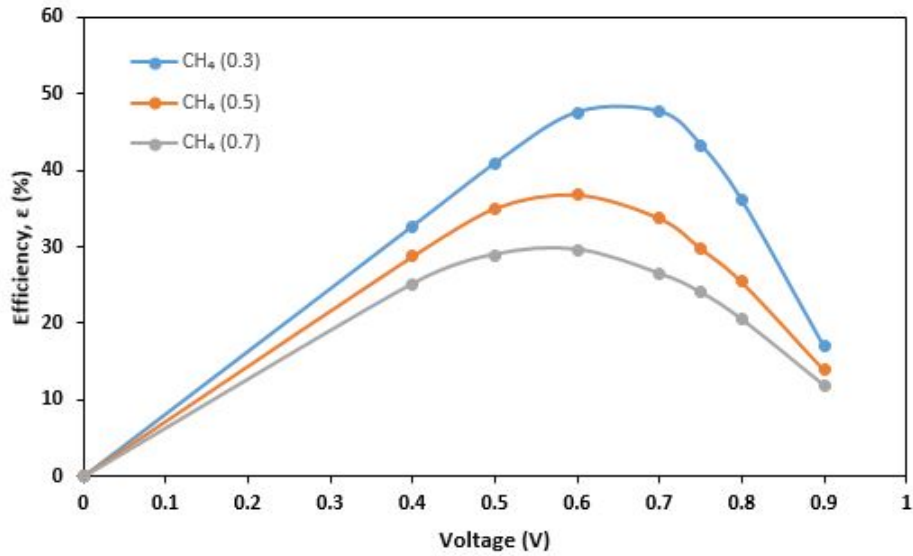


Figure 5.4: Variation of exergy efficiency with mole fraction of CH₄ at 600⁰C

From the Figure 5.4 it is clear that exergy efficiency decreases with mole fraction of CH₄ and shows maximum at 0.3 mole fraction of CH₄. From Table 2.2, it is clear that standard chemical exergy of CH₄ is more than that of H₂O. Because of this as the mole fraction of CH₄ increases, exergy of reactants increases which leads to reduction in exergy efficiency at higher mole fractions of CH₄.

Exergy analysis is also done at 700⁰C and 800⁰C. The performance of SOFC can be greatly improved at higher temperatures. As the temperature increases exergy of reactants and products increases due to increase in physical and chemical exergy. Also at high temperature reaction kinetics will be improved which leads to increase of power.

The exergy efficiency of SOFC at 700⁰C and 800⁰C are shown in Fig. 5.5 and Fig. 5.6 respectively.

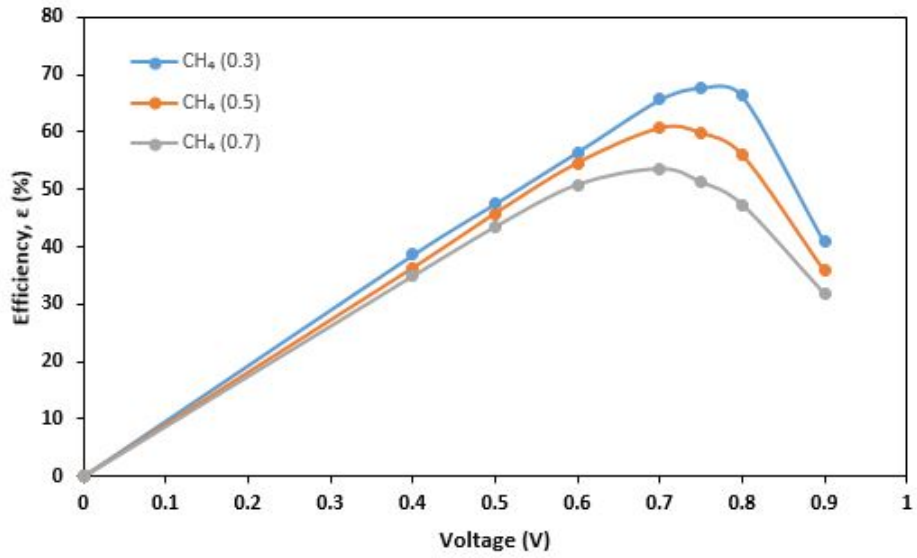


Figure 5.5: Variation of exergy efficiency with mole fraction of CH₄ at 700⁰C

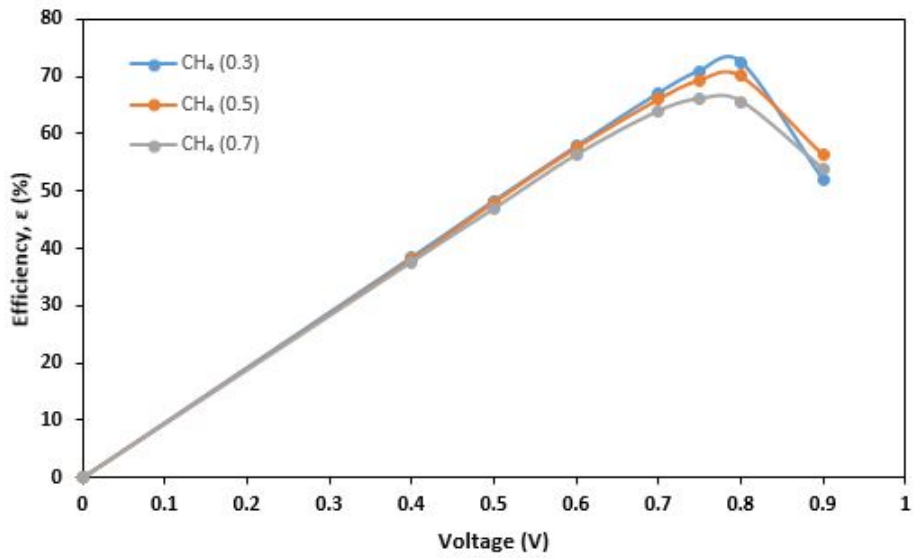


Figure 5.6: Variation of exergy efficiency with mole fraction of CH₄ at 800⁰C

The exergy efficiency is maximum at 800⁰C due to above mentioned reasons. The variation of exergy efficiency at different temperatures at 0.3 mole fraction of CH₄ is shown in Fig. 5.7.

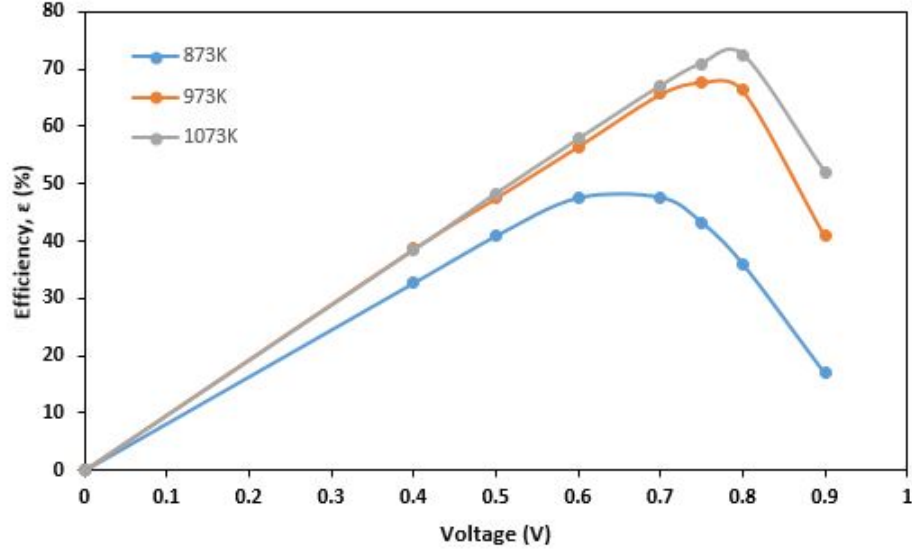


Figure 5.7: Variation of exergy efficiency with temperature at 0.3 mole fraction of CH_4

From the Figure 5.7 it is clear that the maximum exergy efficiency can be obtained at 0.3 mole fraction of CH_4 in the range of 0.7V to 0.8V.

5.2 Efficiency at constant flow rate

Fuel cell is run at different temperatures in constant flow rate condition to determine the efficiency of the fuel cell. To do this, the mole fraction of CH_4 is varied from 0.3 to 0.7 at 0.2 increment with the operating voltage.

The fuel inlet molar flow rate is kept constant at $3.36\text{E-}08$ mol/s and the air molar flow rate is kept constant at $3.23\text{E-}06$ mol/s. At 873K, the velocity of fuel is adjusted to 24.4 cm/s and the velocity of air inlet is adjusted to 812.78 cm/s to match with the total molar flow rates at fuel inlet and air inlet respectively. At 973K, the velocity of fuel is adjusted to 27.2 cm/s and the velocity of air is adjusted to 906.0 cm/s. Similarly, at 1073K, the velocity of fuel and air are adjusted to 30.0 cm/s and 998.96 cm/s respectively. The velocities of fuel and air at different temperatures are shown in Table.5.1. below.

Table 5.1: Velocities at different temperatures

S.No	Temperature (K)	Fuel Velocity (cm/s)	Air Velocity (cm/s)
1.	873	24.4	812.78
2.	973	27.2	906.0
3.	1073	30.0	998.96

At constant flow rate condition, the fuel cell efficiency is given as

$$\eta = (E_{\text{thermo}})(E_{\text{voltage}})(E_{\text{fuel}}). \quad (5.2)$$

Where E_{thermo} , E_{voltage} and E_{fuel} are is reversible thermodynamic efficiency of fuel cell, voltage efficiency of fuel cell and fuel utilization efficiency of fuel cell.

$$E_{\text{thermo}} = \frac{\Delta G}{\Delta H}. \quad (5.3)$$

$$E_{\text{voltage}} = \frac{V}{E}. \quad (5.4)$$

$$E_{\text{fuel}} = \frac{i/nF}{\nu_{\text{fuel}}}. \quad (5.5)$$

For constant flow rate condition,

$$\eta = \left[\frac{\Delta G}{\Delta H} \right] \left[\frac{V}{E} \right] \left[\frac{i/nF}{\nu_{\text{fuel}}} \right]. \quad (5.6)$$

$$\Delta G = nFE. \quad (5.7)$$

After substitution of Eq. 5.6 in Eq. 5.5,

$$\eta = \frac{Vi}{(\Delta H)(\nu_{\text{fuel}})}. \quad (5.8)$$

The analysis involves varying the operating voltage by keeping the mole fraction of CH_4 as constant. This process is continued for mole fractions of CH_4 from 0.3 to 0.7 with an increment of 0.2.

At every temperature the general trend is the same. As the operating voltage increases, the efficiency increases reaches maximum and then decreases. Also, as the mole fraction of CH_4 increases, the efficiency decreases. The reason for this is explained as follows: From the Eq. 5.8, it is clear that as molar flow rate (ν_{fuel}) is constant and the only variables are voltage (V), current and enthalpy of the reaction (Eq. 4.1). As the mole fraction of CH_4 increases the enthalpy of the reaction (Eq. 4.1) increases as shown in the Table 5.2. Therefore as the mole fraction of the CH_4 increases the efficiency decreases as shown in Fig. 5.1 - 5.3 at 600°C , 700°C and 800°C respectively.

Table 5.2: Enthalpy change at different mole fractions

S.No.	Mole fraction of CH_4	Enthalpy change(kJ/mol)		
		600°C	700°C	800°C
1.	0.3	-240.168	-240.322	-240.524
2.	0.5	-400.28	-400.537	-400.874
3.	0.7	-560.391	-560.751	-561.224

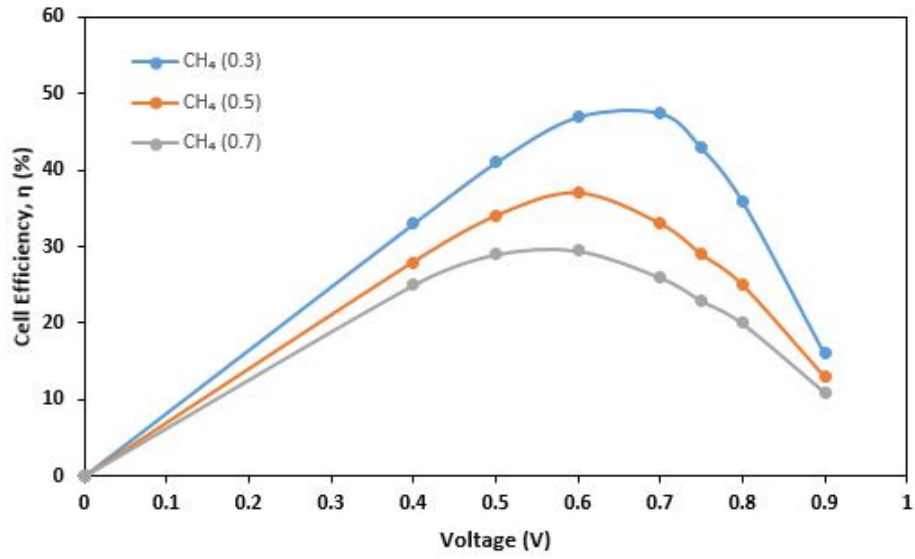


Figure 5.8: Efficiency at constant flow rate at 600⁰C

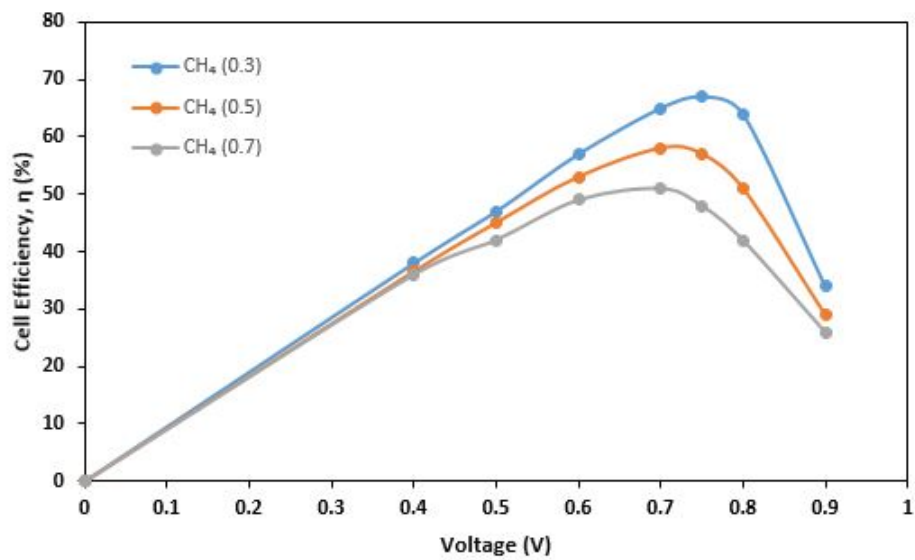


Figure 5.9: Efficiency at constant flow rate at 700⁰C

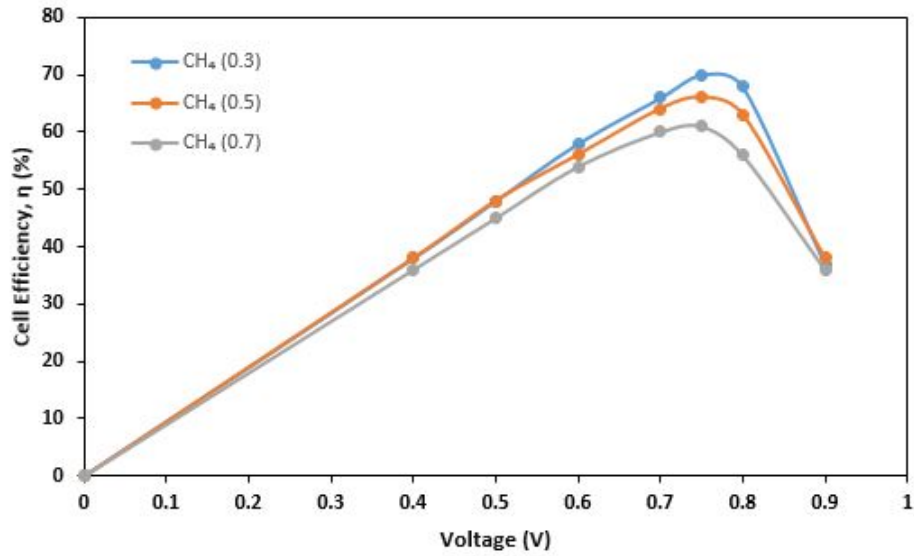


Figure 5.10: Efficiency at constant flow rate at 800⁰C

As the mole fraction of CH₄ increases the fuel cell efficiency decreases due to above mentioned reason. This can be proved by observing the trend of fuel utilization efficiency within the cell. As the mole fraction of CH₄ increases fuel cell utilization decreases as shown in Fig. 5.11 - 5.13 at 600⁰C, 700⁰C and 800⁰C respectively. Due to fuel utilization efficiency is a part of fuel cell efficiency, decrease in utilization efficiency leads to decrease in fuel cell efficiency. Fuel utilization is a function of operating cell voltage for given fuel stream. At low cell potential, the fuel can be utilized fully and fuel-cell efficiency is a liner function of operating voltage. The efficiency reaches a maximum at an operating potential of 0.7V to 0.8V. At low cell voltage, the efficiency increases linearly. In this region the fractional fuel utilization is nearly 1. At around 0.7V the utilization begins to fall, contributing to a decreasing efficiency. The utilization efficiency decreases due to fact that the operating voltage exceeds the reversible voltage of the partially depleted fuel stream. At high voltage, utilization decreases to zero due to none of the fuel can be electrochemically oxidized [19].

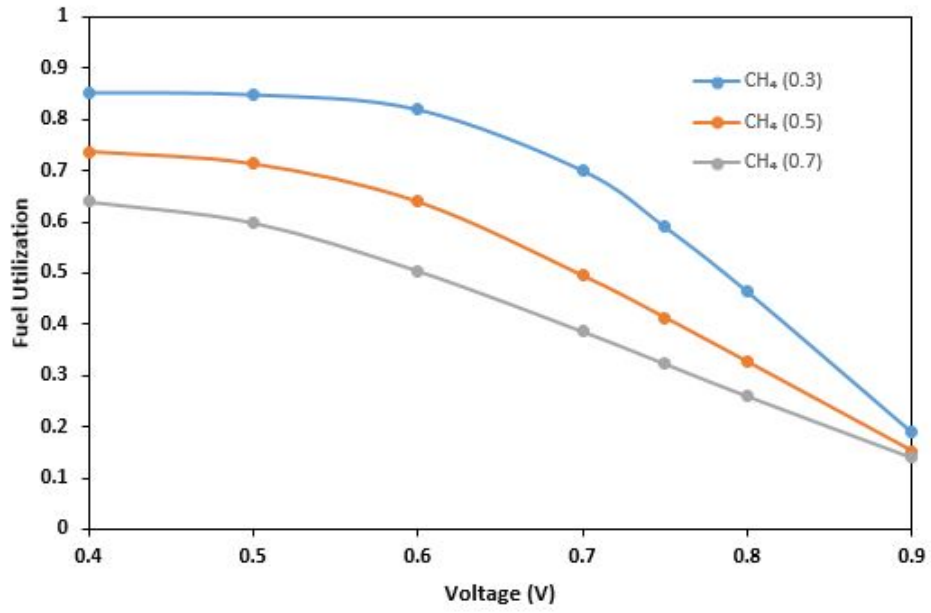


Figure 5.11: Variation of fuel utilization at different mole fractions of CH₄ at 600°C

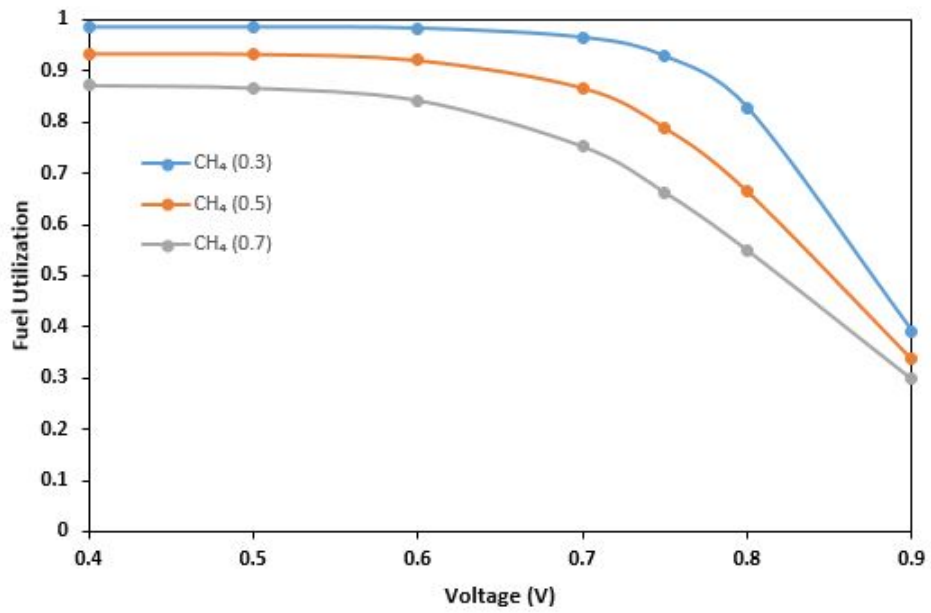


Figure 5.12: Variation of fuel utilization at different mole fractions of CH₄ at 700°C

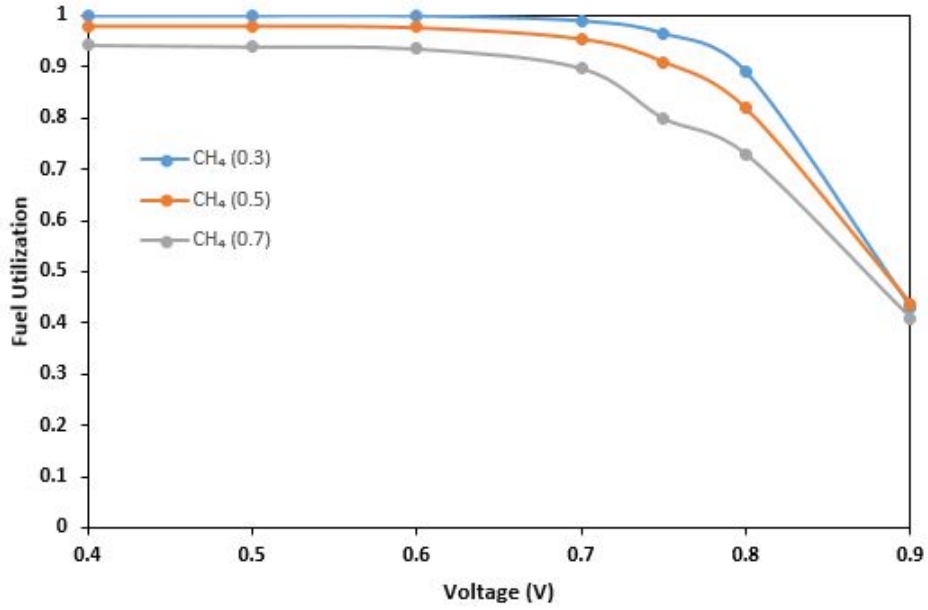


Figure 5.13: Variation of fuel utilization at different mole fractions of CH₄ at 800⁰C

At constant flow rate condition, the maximum efficiency can be achieved at 0.3 mole fraction of CH₄. So mole fraction of CH₄ is taken as the reference to compare the efficiency at different temperatures. Here mole fraction of CH₄ is kept constant at 0.3 and efficiency trend is compared at 600⁰C, 700⁰C and 800⁰C as shown in Fig. 5.14. It can be noted that the efficiency is improved as the temperature is increased. The reason for this trend is as follows: Again referring to the Eq. 5.8, it is cleared that molar flow rate is constant and enthalpy change is insignificant (Table 5.2). The variables are voltage and current density. As the temperature is increased, it improves the kinetics of the reaction which results in increase of power. So the highest efficiency can be obtained at 1073K.

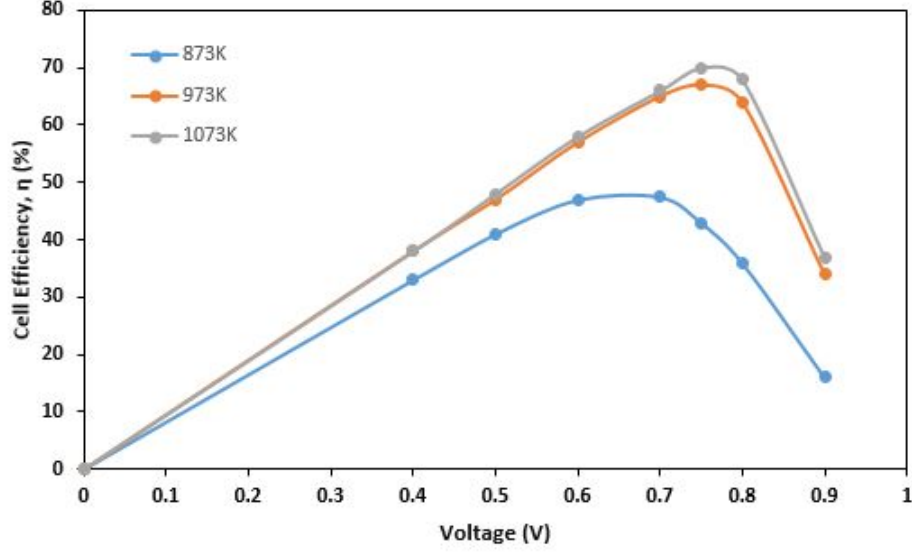


Figure 5.14: Efficiency at constant flow rate at different temperatures

5.3 Efficiency at constant stoichiometry

Fuel cell can be operated in either a constant flow rate condition or a constant stoichiometry condition. In constant stoichiometry condition, supply of fuel to the fuel cell is adjusted to the current such that fuel cell is always supplied with a bit more fuel than it needs. For this work fuel cell is supplied with 1.2 times more fuel than would be required for 100 percent fuel utilization. In constant stoichiometry condition, fuel utilization is independent of current and fuel utilization efficiency is given by

$$E_{\text{fuel}} = \frac{1}{\lambda} \quad (5.9)$$

Where λ is stoichiometric factor.

After substituting Eq. 5.9 into Eq. 5.2,

For constant stoichiometry condition,

$$\eta = \left[\frac{\Delta G}{\Delta H} \right] \left[\frac{V}{E} \right] \left[\frac{1}{\lambda} \right]. \quad (5.10)$$

Fuel cell efficiency at constant stoichiometry condition at 800⁰C is shown in Fig. 5.15

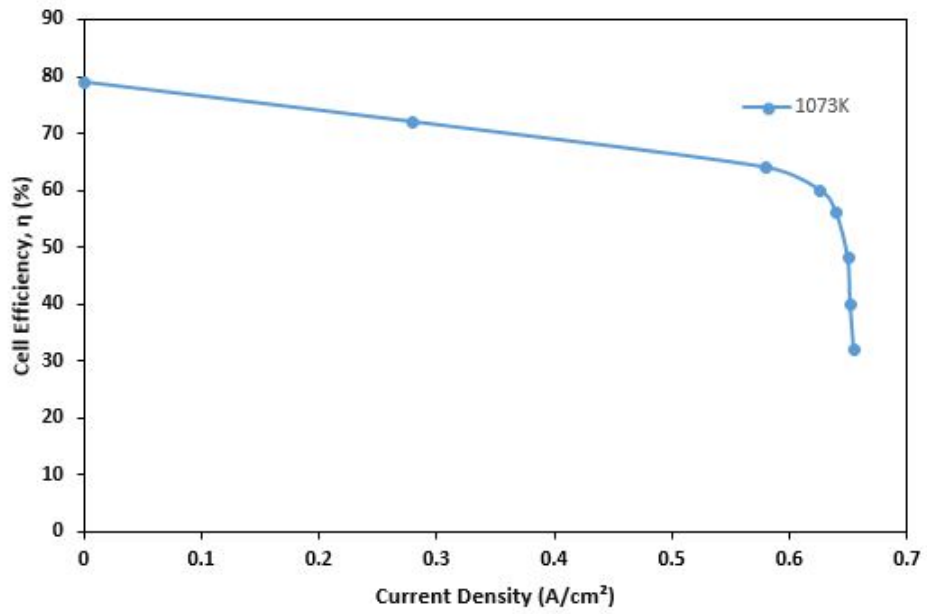


Figure 5.15: Efficiency at constant stoichiometry condition at 800⁰C

Unlike constant flow rate condition, efficiency is maximum at low current density in constant stoichiometry condition.

Chapter 6

Conclusions

Exergy analysis is done on HT - PEMFC to identify the exergy destructions and exergy losses with in the equipments. Most of the exergy losses are identified in equipments like Steam generator, 1st cogeneration, 2nd cogeneration and SMR/WGR cooler. This could help in the improvement of efficiency of the equipments by modify the process path which leads to improved performance of the entire system.

Exergy analysis is done on SOFC at variable operating temperatures, mole fraction of CH₄ and cell voltages. Fuel cell is run at different operating voltages keeping the mole fraction of CH₄ as constant for a particular temperature. This process is repeated for different mole fractions of CH₄. This helped to identify the operating voltage and mole fraction of CH₄ of the fuel cell at which the exergy efficiency is maximum. It is found that operating the fuel cell between 0.7 to 0.8V and 0.3 mole fraction of CH₄ gives the best performance. Also fuel cell is run at different temperatures to determine the performance of it. It is found that as the temperature is increased, the performance of fuel cell is increased and the maximum exergy efficiency can be achieved by operating the fuel cell at 800°C.

In additional to exergy analysis, fuel cell is run at constant flow rate condition to validate the exergy analysis. The analysis of efficiency at constant flow rate condition is in line with exergy analysis.

Bibliography

- [1] Patrick Grimes. Historical pathways for fuel cells. the new electric century. In *Battery Conference on Applications and Advances, 2000. The Fifteenth Annual*, pages 41–45. IEEE, 2000.
- [2] A Boudghene Stambouli and E Traversa. Solid oxide fuel cells (sofcs): a review of an environmentally clean and efficient source of energy. *Renewable and sustainable energy reviews*, 6(5):433–455, 2002.
- [3] AJ Appleby. From sir william grove to today: fuel cells and the future. *Journal of Power Sources*, 29(1-2):3–11, 1990.
- [4] Charles Stone and Anne E Morrison. From curiosity to “power to change the world®”. *Solid State Ionics*, 152:1–13, 2002.
- [5] Fengzhen Chen, TRC Fernandes, Maria Yetano Roche, and Maria da Graça Carvalho. Investigation of challenges to the utilization of fuel cell buses in the eu vs transition economies. *Renewable and Sustainable Energy Reviews*, 11(2):357–364, 2007.
- [6] Dickon Ross. Power struggle [power supplies for portable equipment]. *Iee Review*, 49(7):34–38, 2003.
- [7] José Manuel Andújar and Francisca Segura. Fuel cells: History and updating. a walk along two centuries. *Renewable and sustainable energy reviews*, 13(9):2309–2322, 2009.
- [8] Ryan O’hayre, Suk-Won Cha, Fritz B Prinz, and Whitney Colella. *Fuel cell fundamentals*. John Wiley & Sons, 2016.
- [9] Christopher K Dyer. Fuel cells for portable applications. *Journal of Power Sources*, 106(1-2):31–34, 2002.
- [10] Andrew Dicks and David Anthony James Rand. *Fuel cell systems explained*. 2000.
- [11] Krishnan Sankaranarayanan, Hedzer J Van Der Kooi, and Jakob de Swaan Arons. *Efficiency and sustainability in the energy and chemical industries: scientific principles and case studies*. Crc Press, 2010.
- [12] Ayoub Kazim. Exergy analysis of a pem fuel cell at variable operating conditions. *Energy conversion and management*, 45(11-12):1949–1961, 2004.
- [13] J Szargut. Appendix 1. *Standard chemical exergy, Egzergia. Poradnik obliczania I stosowania, Gliwice: Wydawnictwo Politechniki Shlaskej*, 2007.

- [14] Michael J Moran, Howard N Shapiro, Daisie D Boettner, and Margaret B Bailey. *Fundamentals of engineering thermodynamics*. John Wiley & Sons, 2010.
- [15] Jianlu Zhang, Zhong Xie, Jiujun Zhang, Yanghua Tang, Chaojie Song, Titichai Navessin, Zhiqing Shi, Datong Song, Haijiang Wang, David P Wilkinson, et al. High temperature pem fuel cells. *Journal of power Sources*, 160(2):872–891, 2006.
- [16] Amrit Chandan, Mariska Hattenberger, Ahmad El-Kharouf, Shangfeng Du, Aman Dhir, Valerie Self, Bruno G Pollet, Andrew Ingram, and Waldemar Bujalski. High temperature (ht) polymer electrolyte membrane fuel cells (pemfc)—a review. *Journal of Power Sources*, 231:264–278, 2013.
- [17] Alexandros Arsalis, Mads P Nielsen, and Søren K Kær. Modeling and off-design performance of a 1 kwe ht-pemfc (high temperature-proton exchange membrane fuel cell)-based residential micro-chp (combined-heat-and-power) system for danish single-family households. *Energy*, 36(2):993–1002, 2011.
- [18] Anusree Unnikrishnan, N Rajalakshmi, and Vinod M Janardhanan. Mechanistic modeling of electrochemical charge transfer in ht-pem fuel cells. *Electrochimica Acta*, 2017.
- [19] Huayang Zhu and Robert J Kee. Thermodynamics of sofc efficiency and fuel utilization as functions of fuel mixtures and operating conditions. *Journal of Power sources*, 161(2):957–964, 2006.